Compact Grating Structure for Application to Filters and Resonators in Monolithic Microwave Integrated Circuits

TE-HUI WANG, STUDENT MEMBER, IEEE, AND TATSUO ITOH, FELLOW, IEEE

Abstract — **Possible high-Q circuits based on a new crosstie overlay slow-wave structure are proposed for monolithic microwave integrated circuits. Configurations and results of slow-wave factors are presented. This structure is used for construction of a frequency-selective reflector with a compact size. The effect of loss is considered.**

I. INTRODUCTION

ONE OF THE PROBLEMS of microwave and millimeter-wave integrated circuits is lack of high-Q resonators except for a dielectric resonator. In monolithic integrated circuits, dielectric resonators are not compatible with the concept of *monolithic* integration. Microstrip patches provide a relatively low Q. In this study, we investigate the possibility of realizing resonators and oscillators, with a reasonable physical size, by the use of grating structures in a printed line form constructed by a new low-loss slow-wave structure.

It is known that a grating structure exhibits the stop-band phenomenon, which can be used as a band-reject filter [1] and as a band-pass filter if combined with a coupler [2]. Several years ago, a Gunn oscillator in the form of a dielectric image guide was reported in which the frequency-selective reflectors were created on both sides of the diode by means of grating structures [3]. The structure was the microwave and millimeter-wave version of DBR (distributed Bragg reflector) laser in optics [4], [5]. Recently, a renewed effort has been reported at the *Ka*-band with good results [6]. The concept of the DBR resonator has also been used in the finline configuration [7]. It was found that the design of the finline Gunn oscillator became more flexible with the use of periodic structures for frequency-selective feedback.

Because the DBR structure is made of a grating, it is electrically long and, hence, is not very suitable for monolithic integrated circuits. In this paper, we propose the use of a slow-wave structure to form a printed line grating so that its physical dimension is more reasonable. Conventional MIS or Schottky slow-wave structures are inherently lossy [8], although the latter can provide the possibility of electronic tuning of oscillation frequency if it is used as a DBR resonator in the form of a periodic structure, provided the attenuation is reasonable. Recently, Hasegawa proposed a new crosstie coplanar waveguide (CPW) slow-wave structure in which the wave attenuation is due only to the conductor loss [8] (Fig. 1). Here we propose a crosstie overlay slow-wave structure (Fig. 2) which is a modification of Hasegawa's structure, but is more adaptable for monolithic circuit integration. Fabrication is easier because we deposit a dielectric overlay and crosstie strips after the CPW or microstrip is fabricated on a GaAs substrate. This new structure can be made free of dielectric loss in principle, if no tuning is required, although minimization of the conductor loss is still important. If tuning is desired, it is possible to combine this new structure with a Schottky slow-wave mechanism by providing a doped layer before the CPW or microstrip is fabricated. In such a

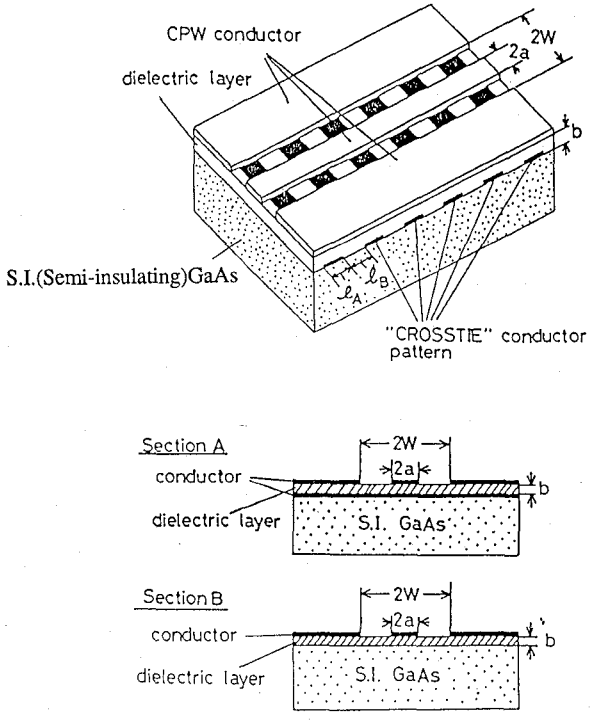

Fig. 1. Crosstie coplanar waveguide (CPW) slow-wave structures (by Hasegawa).

Manuscript received April 7, 1987; revised July 16, 1987. This work was supported in part by the U.S. Army Research Office under Contract DAAG-84-K-0076.

The authors are with the Department of Electrical and Computer Engineering, University of Texas, Austin, TX 78712.

IEEE Log Number 8717117.

0018-9480/87/1200-1176$01.00 ©1987 IEEE

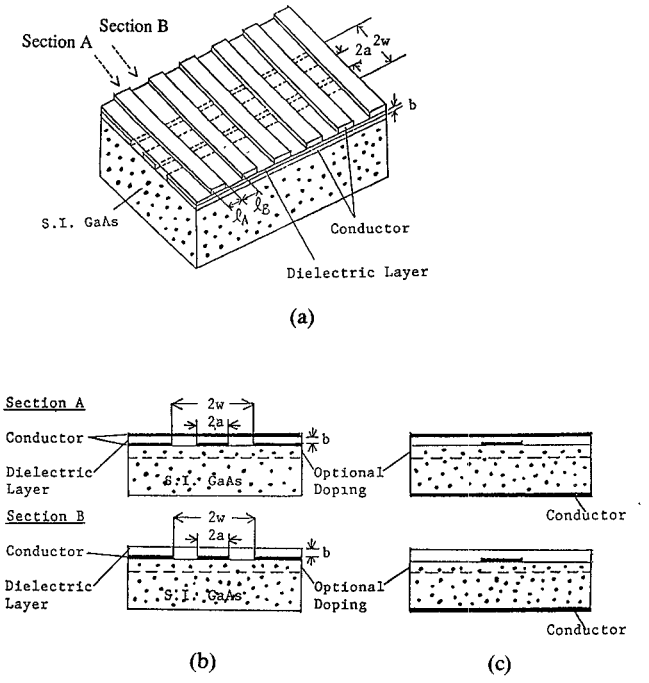

Fig. 2. Crosstie overlay CPW and microstrip slow-wave structures. (a) CPW. (b) Cross sections of CPW. (c) Cross sections of microstrip.

structure, the attenuation introduced by the doped layer should be minimized while some bias tunability of a Schottky slow-wave mechanism is retained. Periodic doping [9] may be one candidate.

In Section II, we study the characteristics of the new crosstie structure as a slow-wave transmission line. Section III describes predicted characteristics of this new slow-wave structure. The effect of conductor loss is included. In Section IV, we consider the use of this slow-wave structure for creation of a grating structure for possible high-Q components such as a band-reject filter. Section V presents predicted results of a band-reject filter.

II. Slow-Wave Principle and Waveguide Structure

The basic operating principle of how the crosstie structure works as a slow-wave transmission line is a spatial separation of electric and magnetic energy. In the section with a crosstie strip, the capacitance is significantly increased, whereas the section with only the dielectric overlay is more inductive. The spatial separation of energy is therefore accomplished in a periodic manner. This structure is essentially a grating. However, we do not use this structure as a grating. By making the period $l_A + l_B$ in Fig. 2 sufficiently smaller than the operating wavelength, the operating point is far away from the stopband and this structure models a uniform transmission line with its propagation constant and characteristic impedance calculable from the periodic dispersion relation.

The theoretical treatment of the new slow-wave CPW consists of using Floquet's theorem for periodic transmission lines. To do this, accurate values of both propagation constants and characteristic impedances of the constituent sections l_A and l_B need to be calculated (see Fig. 2). Using the standard spectral-domain analysis [10], these values can be calculated and the periodic slow-wave CPW can be analyzed. After applying Floquet's theorem and requiring current and voltage continuity at each junction, we obtain the following dispersion and impedance equations:

$$\cosh(\gamma l) = \cosh(\gamma_A l_A)\cosh(\gamma_B l_B) + (1/2) \cdot (z_A/z_B + z_B/z_A)\sinh(\gamma_A l_A)\sinh(\gamma_B l_B) \quad (1)$$

$$Z = \left[z_A \sinh(\gamma_A l_A)\cosh(\gamma_B l_B) + z_B \cosh(\gamma_A l_A)\sinh(\gamma_B l_B)\right]^{1/2} \Big/ \left[(1/z_A)\sinh(\gamma_A l_A)\cosh(\gamma_B l_B) + (1/z_B)\cosh(\gamma_A l_A)\sinh(\gamma_B l_B)\right]^{1/2} \quad (2)$$

$$\gamma = \alpha + j\beta \quad (3)$$

$$\gamma_A = \alpha_A + j\beta_A \quad (4)$$

$$\gamma_B = \alpha_B + j\beta_B \quad (5)$$

where

- α attenuation constant of the crosstie overlay slow-wave CPW's,
- β propagation constant of the crosstie overlay slow-wave CPW's,
- Z characteristic impedance of the crosstie overlay slow-wave CPW's,
- α_A, β_A attenuation constant and propagation constant of section A, respectively,
- α_B, β_B attenuation constant and propagation constant of section B, respectively,
- z_A, z_B characteristic impedances of sections A and B, respectively,
- $l = l_A + l_B$, with l_A and l_B being the lengths of sections A and B, respectively.

In this approach, the effect of the geometrical discontinuity at the junction of two sections is neglected; however, it is assumed to be small.

III. Predicted Results of the Slow-Wave Structure

Fig. 3 shows the normalized propagation constants $\beta_A/\beta_0, \beta_B/\beta_0$ of the constituent sections A and B in the crosstie overlay structure, where β_0 is free-space wavenumber. Curve A corresponds to section A (with a crosstie strip) and curve B is for section B. Fig. 4 shows the characteristic impedances of sections A and B. There exists a significant difference in the characteristic impedance for the two sections, one of which is much more capacitive and the other is more inductive. The data for Figs. 3 and 4 have been calculated by the spectral-domain method. In the spectral-domain method calculation, we assumed that the thicknesses of the conductors in both CPW and crosstie metal strip were infinitesimally thin. Convergence checks showed that 0.5 percent and 1 percent accuracy could be achieved for the propagation constant and the

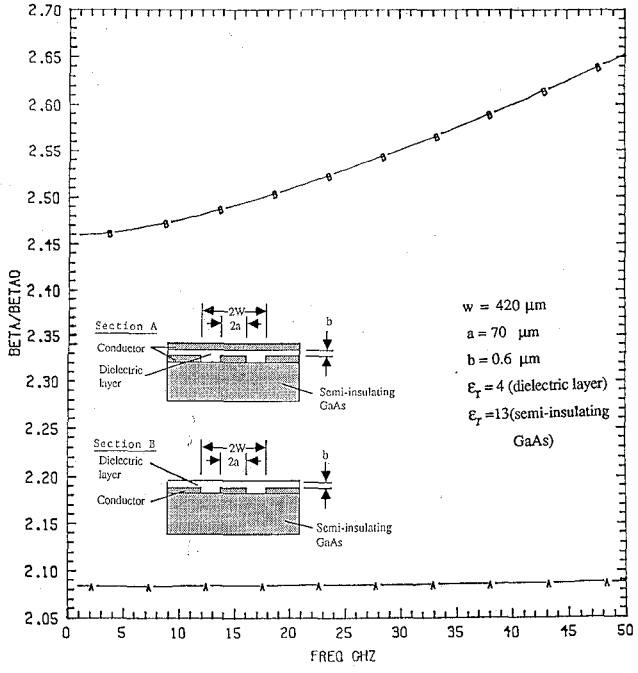

Fig. 3. Normalized propagation constant of slow-wave CPW.

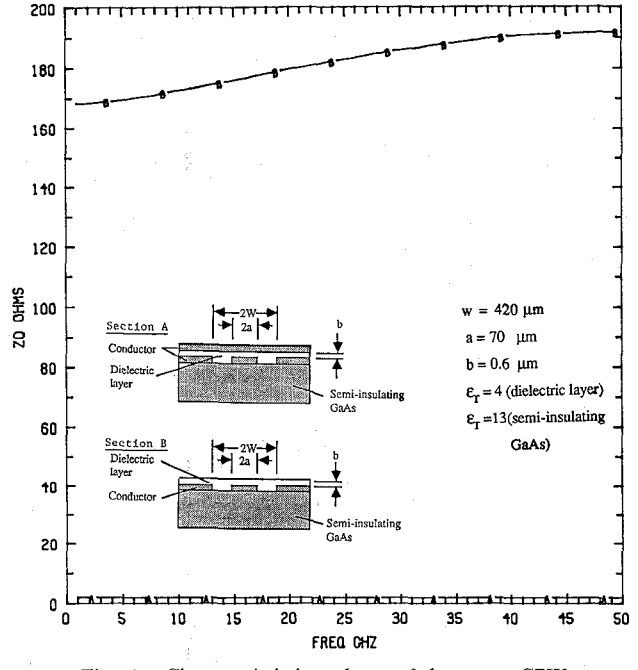

Fig. 4. Characteristic impedance of slow-wave CPW.

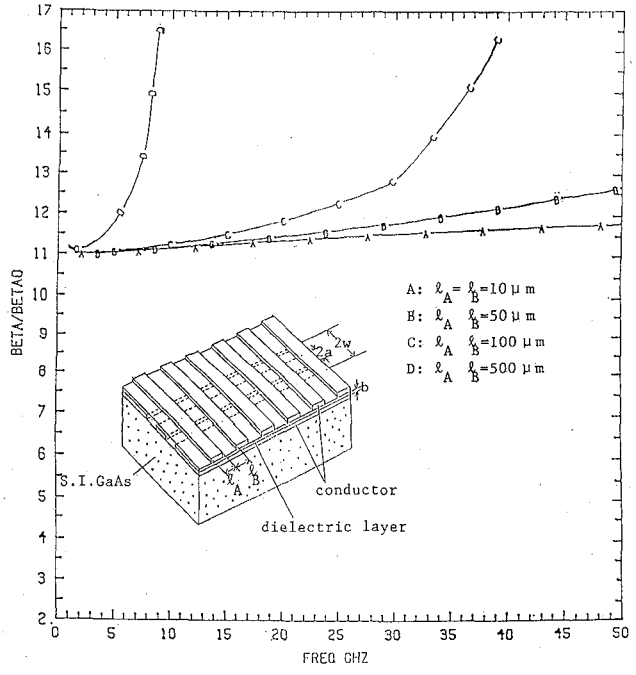

Fig. 5. Normalized propagation constant of periodic slow-wave CPW with different periodicity. $a = 70\ \mu$m, $w = 420\ \mu$m, $b = 0.6\ \mu$m, $\epsilon_r = 4$ (overlay).

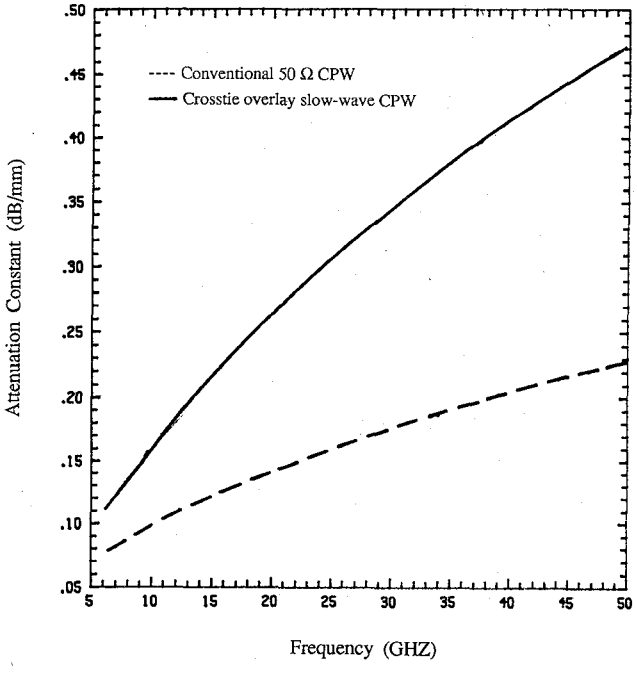

Fig. 6. Conductor loss of the crosstie overlay slow-wave structures.

characteristic impedance, respectively, by using four basis functions in both transverse and longitudinal electric field expansions at the slot regions. Of course, the convergence accuracy could be further enhanced if more basis functions were used.

Fig. 5 shows the dispersion characteristics of the infinitely long crosstie overlay CPW. The information for each constituent section has been used in Floquet's theorem. We then obtain curves in Fig. 5. It is noticed that as the frequency is increased, the curve approaches a very dispersive region, which is caused by the stopband phenomenon. This stopband frequency increases as the length of the grating period is reduced. Therefore, if the period chosen is much smaller than the operating wavelength, the corresponding frequency is at the linear portion of the curve much below the stopband, so that the structure can be viewed as a uniform transmission line. As an example, at the frequency of 20 GHz on curve C in Fig. 5, the slow-wave factor (β/β_0) is 11.6. Fig. 6 shows the attenuation constants (α) due to conductor loss of the crosstie

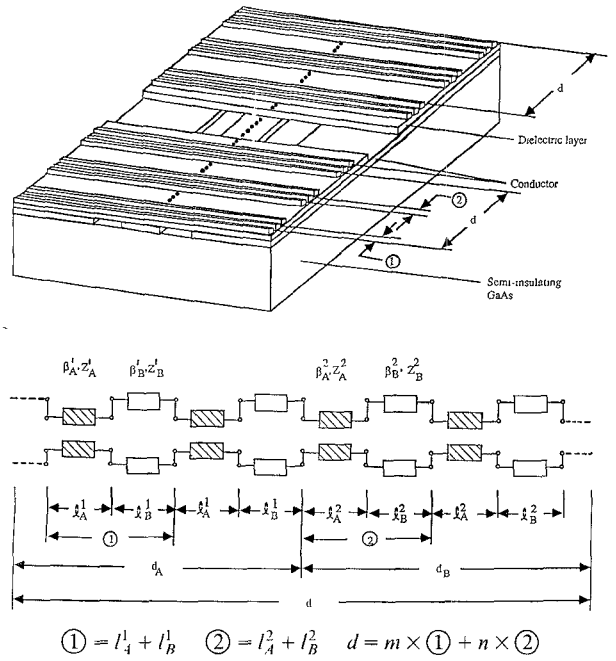

Fig. 7. Schematic feature and equivalent circuit of the crosstie overlay slow-wave grating.

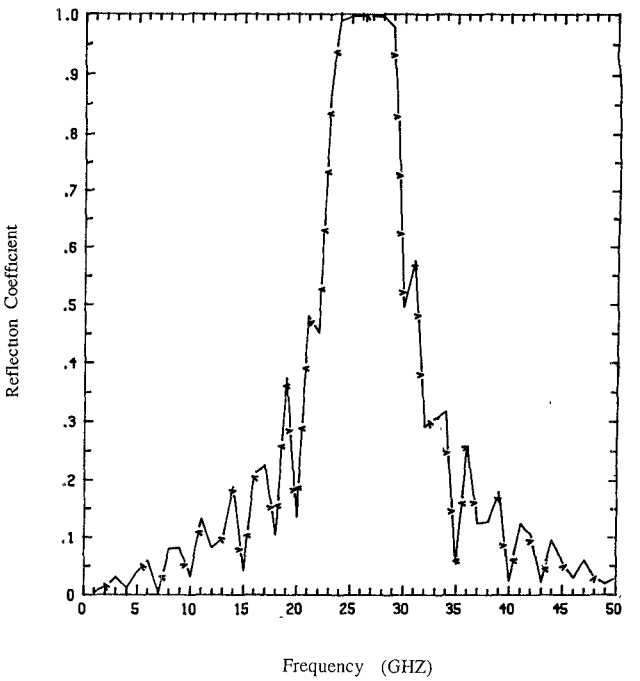

Fig. 8. Reflection coefficient of the crosstie overlay slow-wave grating with lossless conductor.

overlay slow-wave structures along with the conventional 50-Ω CPW transmission line. In this figure, we have assumed that the attenuation constants due to dielectric loss in both sections A and B were negligibly small. Based on Wheeler's incremental inductance formula [11], and gold as the conductor material with a resistivity and a thickness equal to 2.3×10^{-6}Ω-cm and 1 μm, respectively, the attenuation constants due to CPW and crosstie conductor losses in section A (α_A) and due to CPW conductor loss only in section B (α_B) were calculated. In the meantime, we assumed that the propagation constants in section A (β_A) and section B (β_B) were not affected by the attenuation due to conductor loss. By applying (1), we finally obtained the attenuation constant of the infinitely long crosstie overlay slow-wave CPW's. As shown in this figure, the crosstie overlay slow-wave CPW's exhibit higher attenuation per unit length than conventional CPW's due to the existence of the crosstie conductors. However, the attenuation per unit length in the crosstie structure is comparable to that in a 50-Ω CPW. Of course, there may be additional loss due to discontinuities in the crosstie structure. Such an additional loss will be studied in the future.

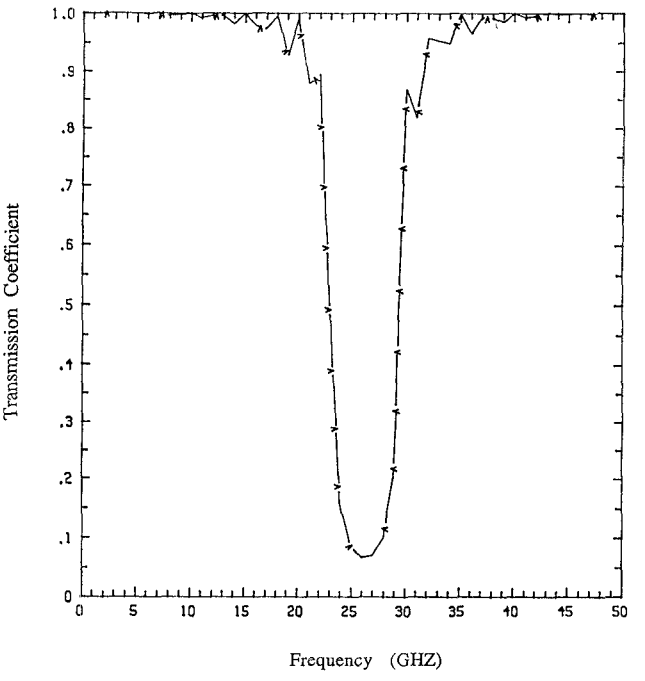

Fig. 9. Transmission coefficient of the crosstie overlay slow-wave grating with lossless conductor.

IV. Grating Structure Made from Crosstie Slow-Wave Structure

As shown in Fig. 7, we create a grating with its period comparable to the guide wavelength from the "uniform" crosstie overlay slow-wave CPW's. As shown in this figure, one period of the grating consists of two sections of crosstie overlay slow-wave CPW's with different slow-wave factors and characteristic impedances. The slow-wave CPW in section d_A comprises sections A and B of lengths 5 μm and 6 μm, respectively, while the one in the section d_B is made of 6 μm and 5 μm long sections. Hence, in reference to Fig. 7, $l_A^1 = 5$ μm and $l_B^1 = 6$ μm while $l_A^2 = 6$ μm and $l_B^2 = 5$ μm. Section d_A contains 20 periods of $l_A^1 + l_B^1$ while d_B contains 20 periods of $l_A^2 + l_B^2$. Hence, the length of the d of the band-reject grating is 440μm. Section d_A has a higher characteristic impedance than section d_B.

To study the band-rejection properties of this grating, the same analysis procedures used in calculating the propagation constant and characteristic impedance for the uni-

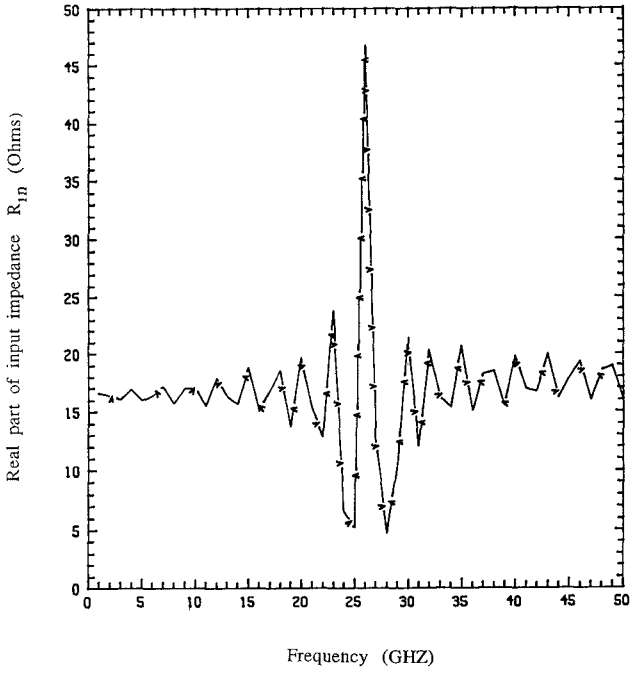

(a)

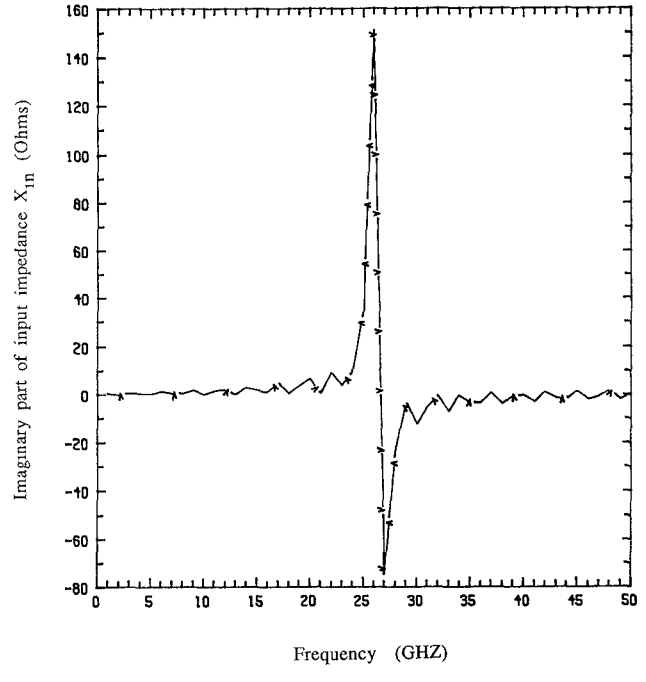

(b)

Fig. 10. (a) Real part of the input impedance of the crosstie overlay slow-wave grating with lossless conductor. (b) Imaginary part of the input impedance of the overlay crosstie slow-wave grating with lossless conductor.

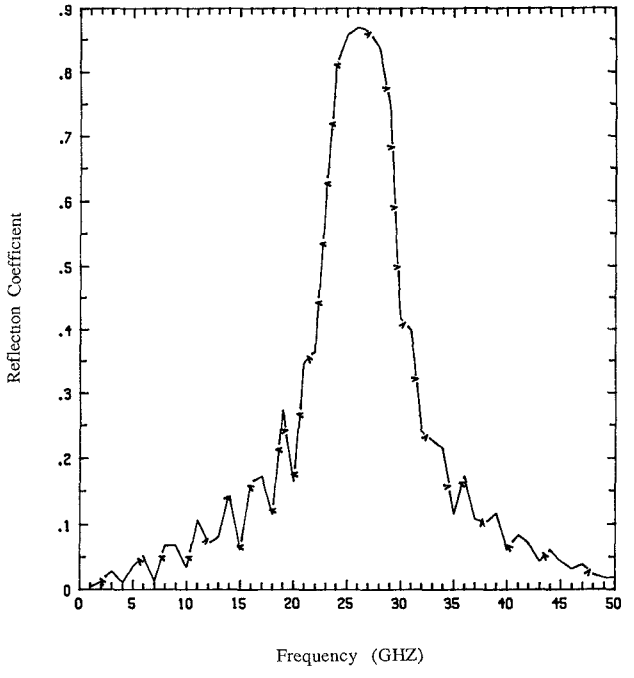

Fig. 11 Reflection coefficient of the crosstie overlay slow-wave grating with lossy conductor.

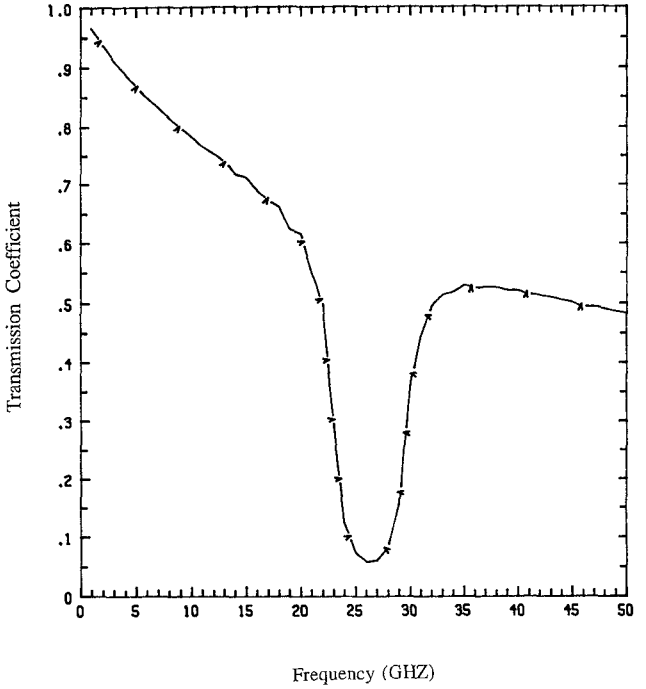

Fig. 12. Transmission coefficient of the crosstie overlay slow-wave grating with lossy conductor.

form crosstie slow-wave CPW's are employed to obtain the transmission characteristics of the constituent sections $l_A^1 + l_B^1$ and $l_A^2 + l_B^2$ in Fig. 7. Once the propagation constants and characteristic impedances of the two constituent crosstie slow-wave structures are obtained, appropriate lengths of the two sections d_A and d_B are chosen and cascaded to form a period of the band-reject grating, as described in the previous paragraph. The reflection and transmission performances are then characterized by using the microwave two-port network cascading technique.

V. Results of Grating Made from New Slow-Wave Structures

Figs. 8 and 9 are the reflection and transmission coefficients, respectively, of the wave incidence into a band-reject grating. This grating consists of nine periods plus one

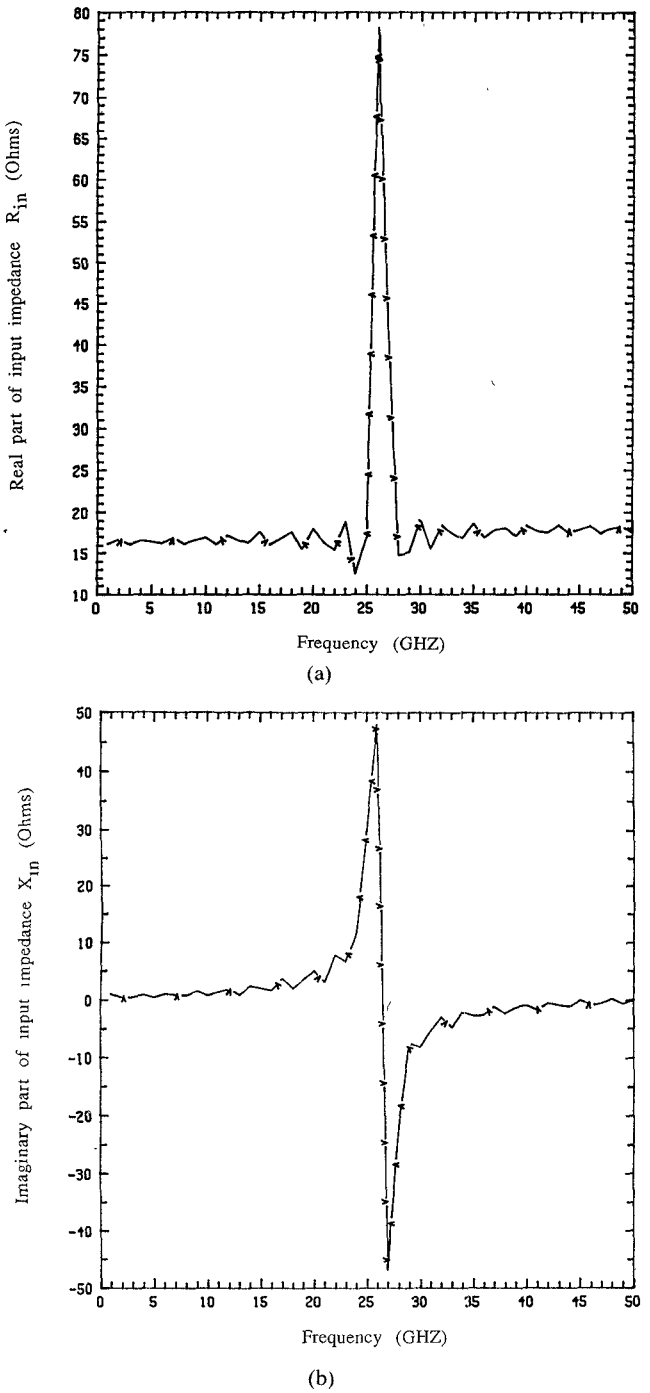

Fig. 13. (a) Real part of the input impedance of the crosstie overlay slow-wave grating with lossy conductor. (b) Imaginary part of the input impedance of the crosstie overlay slow-wave grating with lossy conductor.

section, d_A, so that the structure is directionally symmetric. The physical length of this grating is 4.18 mm. The load impedance connecting to the output end of the grating is 16 Ω. The center frequency of the stopband is about 26 GHz. Figs. 10(a) and 10(b) are the real and imaginary parts of the input impedance of the grating. In the calculation for Figs. 8, 9, and 10, the conductor loss has been neglected.

To study how the wave attenuation due to the conductor loss affects this grating performance, we evaluated the reflection and transmission characteristics of the 4.18-mm grating structure in the presence of conductor loss. Based on the incremental inductance approach, the attenuation constants were calculated for every constituent section of the grating. The results have then been used in the calculation of the reflection and transmission characteristics. Figs. 11 and 12 are the reflection and transmission coefficients of the 4.18-mm grating after taking the conductor loss into account. Due to the conductor loss, the peak of the reflection coefficient has been reduced from 0.998 to 0.875. Figs. 13(a) and 13(b) are the real and imaginary parts of the grating after taking the conductor loss into account.

It is well known that the "sidelobes" can be eliminated if we use a weight taper in the grating. In addition, the reflection coefficient can be enhanced and the stopband width can also be shrunk if the band-rejection properties of the grating have been optimized. We are currently working on these problems.

VI. Conclusions

A new slow-wave grating structure is proposed which has the possibility of being used as band-reject and band-pass filters and resonators with a reasonable physical size. Respectable slow-wave factors and promising bandstop phenomena are obtained. The effect of the conductor loss has been taken into account. This structure can also be used in a frequency-selective distributed Bragg reflection (DBR) Gunn oscillator in a planar circuit form.

References

[1] T. Itoh, "Application of grating in a dielectric waveguide for leaky-wave antennas and band-reject filters," *IEEE Trans. Microwave Theory Tech.*, vol. MTT-25, pp. 1134–1138, Dec. 1977.

[2] P. K. Ikalainen, G. L. Matthaei, D. C. Purk, and M. S. Wei, "Dielectric waveguide band-pass filters with broad stop bands," in *1985 IEEE MTT-S Int. Microwave Symp.* (St. Louis, MO), June 4–6, 1985, pp. 277–280.

[3] T. Itoh and F.-J. Hsu, "Distributed Bragg reflection Gunn oscillators for dielectric millimeter-wave integrated circuits," *IEEE Trans. Microwave Theory Tech.*, vol. MTT-27, pp. 514–518, May 1979.

[4] S. Wang, "Principles of distributed feedback and distributed Bragg reflection lasers," *IEEE J. Quantum Electron.*, vol. QE-10, pp. 413–427, Apr. 1974.

[5] W. Streifer, D. R. Scifres, and R. D. Burnham, "Coupled wave analysis of DFB and DBR lasers," *IEEE J. Quantum Electron.*, vol. QE-13, p. 134–141, Apr. 1977.

[6] Z.-W. Li and W.-X. Zhang, "Design and performance of the millimeter wave DBR Gunn oscillators, in *1986 IEEE MTT-S Int. Microwave Symp.* (Baltimore, MD), June 2–4, 1986, pp. 531–534.

[7] H. Hofmann, "MM-wave Gunn oscillator with distributed feedback fin-line circuit," in *1980 IEEE MTT-S Int. Microwave Symp.* (Washington, DC), May 28–30, 1980, pp. 59–61.

[8] S. Seki and H. Hasegawa, "Cross-tie-slow-wave coplanar waveguide on semi-insulating GaAs substrate," *Electron. Lett.*, vol. 17, no 25, pp. 940–941, Dec. 10, 1981.

[9] Y. Fukoka and T. Itoh, "Slow-wave coplanar waveguide on periodically doped semiconductor substrate," *IEEE Trans. Microwave Theory Tech.*, vol. MTT-31, pp. 1013–1017, Dec. 1983.

[10] T. Itoh, "Spectral domain immittance approach for dispersion characteristics of generalized printed transmission lines," *IEEE Trans. Microwave Theory Tech.*, vol. MTT-28, pp. 733–736, July 1980.

[11] H. A. Wheeler, "Transmission-line properties of parallel strips separated by a dielectric sheet," *IEEE Trans. Microwave Theory Tech.*, vol. MTT-13, pp. 172–185, Mar. 1965.

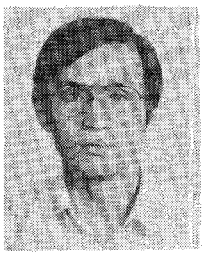

Te-Hui Wang (S'86) was born in Taichung, Taiwan, R.O.C., on May 16, 1954. He received the B.Sc. degree in physics from National Tsing Hua University, Taiwan, in 1977, and the M.E. degree in electrical engineering from the Tatung Institute of Technology, Taiwan, in 1981.

From 1981 to 1985, he was with the Chung Shun Institute of Science and Technology, Lung Tan, Taiwan, serving as an assisting scientist. He has been involved in the research and development of microwave semiconductor devices. Since 1985, he has been on leave from his position there to pursue the Ph.D. degree at the University of Texas at Austin. His current research interests includes the analysis and design of microwave and millimeter-wave components.

✠

Tatsuo Itoh (S'69–M'69–SM'74–F'82) received the Ph.D. degree in electrical engineering from the University of Illinois, Urbana, in 1969.

From September 1966 to April 1976, he was with the Electrical Engineering Department, University of Illinois. From April 1976 to August 1977, he was a Senior Research Engineer in the Radio Physics Laboratory, SRI International; Menlo Park, CA. From August 1977 to June 1978, he was an Associate Professor at the University of Kentucky, Lexington. In July 1978, he joined the faculty at the University of Texas at Austin, where he is now a Professor of Electrical and Computer Engineering and Director of the Electrical Engineering Research Laboratory. During the summer of 1979, he was a guest researcher at AEG-Telefunken, Ulm, West Germany. Since September 1983, he has held the Hayden Head Centennial Professorship of Engineering at the University of Texas. Since September 1984, he has been Associate Chairman for Research and Planning of the Electrical and Computer Engineering Department.

Dr. Itoh is a member of the Institute of Electronics and Communication Engineers of Japan, Sigma Xi, and Commission B of USNC/URSI. He served as Editor of the IEEE TRANSACTIONS ON MICROWAVE THEORY AND TECHNIQUES from 1983 to 1985. Dr. Itoh serves on the Administrative Committee of the IEEE Microwave Theory and Techniques Society. He is a Professional Engineer registered in the state of Texas.